

Manifestation of Spin Selection Rules on the Quantum Tunneling of Magnetization in a Single Molecule Magnet

J. J. Henderson¹, C. Koo², P. L. Feng³, E. del Barco^{1,*}, S. Hill⁴, I. S. Tupitsyn⁵, P. C. E.
Stamp⁵ and D. N. Hendrickson³

¹*Department of Physics, University of Central Florida, Orlando, FL 32816, USA*

²*Department of Physics, University of Florida, Gainesville, FL32611, USA*

³*Department of Chemistry and Biochemistry, University of California at San Diego, La Jolla, CA
92093, USA*

⁴*National High Magnetic Field Laboratory and Department of Physics, Florida State University,
Tallahassee, FL 32310, USA*

⁵*Pacific Institute for Theoretical Physics, University of British Columbia, 6224 Agricultural
Road, Vancouver, B.C., Canada, V6T 1Z1*

**Electronic mail: delbarco@physics.ucf.edu*

ABSTRACT:

We present low temperature magnetometry measurements on a new Mn₃ single-molecule magnet (SMM) in which the quantum tunneling of magnetization (QTM) displays clear evidence for quantum mechanical selection rules. A QTM resonance appearing only at high temperatures demonstrates tunneling between excited states with spin projections differing by a multiple of three. This is dictated by the C₃ molecular symmetry, which forbids pure tunneling from the lowest metastable state. Transverse field resonances are understood by correctly orienting the Jahn-Teller axes of the individual manganese ions, and including transverse dipolar fields. These factors are likely to be important for QTM in *all* SMMs.

Observations of basic quantum phenomena in single-molecule magnets (SMMs) [1-12] and their potential for quantum information technologies [3] have resulted in a much better understanding of magnetization dynamics in nanoscale systems. In the bottom-up approach of supramolecular chemistry, the quantum properties of SMMs are dictated by molecular composition and configuration: molecular and crystallographic symmetries then play an essential role in the tunneling dynamics. An elegant example is provided by Berry phase interference between different tunneling trajectories, determined by anisotropy terms in the Hamiltonian directly imposed by molecular symmetry [7,10].

Crucially, symmetry also enforces spin selection rules in tunneling, only allowing transitions with a change of spin projection, $|\Delta m_S|$, equal to the order of the spin ladder operators in the transverse anisotropy terms in the Hamiltonian (in zero transverse field). Thus, e.g., molecules with S_4 symmetry (e.g. $\text{Mn}_{12}\text{tBuAc}$; tetragonal crystal lattice), only allow $|\Delta m_S| = 4n$, where n is an integer; and molecules with C_3 (e.g. Mn_3 [13-19]; trigonal lattice) or D_2 (e.g. Fe_8 ; triclinic lattice) symmetries only permit $|\Delta m_S| = 3n$ and $2n$, respectively. Surprisingly, in all experimental studies on SMMs to date, QTM is found at all resonances, in spite of these selection rules (of which only subtle manifestations have been reported so far [7,20,21]). There are many possible reasons for this: (i) Intrinsic disorder (from solvent loss, ligand disorder or crystal defects) lowers the local symmetry, so that an applied longitudinal field induces a distribution of transverse magnetic field components [8-10], (ii) dynamic fields from nuclear spins [11], (iii) dipolar interactions [22], and (iv) internal transverse fields. Lacking so far is a clear-cut experimental demonstration of how molecular symmetry controls QTM, in which all these extraneous effects are either eliminated or accounted for.

In this Letter we present such a demonstration, using a high-quality crystal of a Mn_3 complex. The crystalline quality is demonstrated by the unsurpassed sharpness of the X-ray diffraction and EPR absorption peaks [13,14]. We observe a sequence of very sharp QTM steps, with one resonance appearing only at high temperature. The high-T relaxation at this resonance comes from transitions involving excited states with $|\Delta m_S| = 3n$, dictated by the C_3 molecular symmetry (which forbids tunneling from the lowest metastable state). In addition, a rotation of the local zero-field-splitting (ZFS) tensors following the tilts of the Jahn-Teller axes of the Mn^{III} ions, in combination with intermolecular dipolar interactions, accounts for the observed behavior in all QTM resonances, including transitions nominally forbidden by the molecular symmetry.

We have studied the two complexes $[\text{NEt}_4]_3[\text{Mn}_3\text{Zn}_2(\text{salox})_3\text{O}(\text{N}_3)_6\text{Cl}_2]$ and $[\text{NEt}_4]_3[\text{Mn}_3\text{Zn}_2(\text{salox})_3\text{O}(\text{N}_3)_6\text{Br}_2]$, henceforth $\text{Mn}_3\text{-Cl}$ and $\text{Mn}_3\text{-Br}$, respectively [13,14]. Their metallic cores contain a μ_3 -oxo-centered triangle of Mn^{3+} ions plus two capping Zn^{2+} ions above and below the Mn_3 plane, giving a rigid trigonal bipyramidal structure. The diamagnetic Zn^{2+} ions and bulky $[\text{NEt}_4]^+$ cations isolate the Mn_3 core from intermolecular magnetic interactions, as evident from the absence of significant intermolecular contacts and the 10.30 Å minimum separation between Mn^{III} ions in neighboring molecules. Both complexes crystallize in the trigonal space group $R3c$ as equally-populated racemic mixtures of C_3 -symmetric chiral molecules (with opposite chiralities rotated by 27 degrees about the C_3 axis with respect to each other). Neither structure contains solvate molecules, which is quite rare for SMMs and likely explains the extremely high resolution spectroscopic data (solvents evaporate easily, causing disorder [23]). Ferromagnetic exchange interactions between Mn^{3+} ions act via the central

μ_3 -oxo ion and the coordinating oxime, resulting in a molecular spin $S = 6$ ground state. These structural and crystallographic properties differentiate $\text{Mn}_3\text{-Cl}$ and $\text{Mn}_3\text{-Br}$ from other ferromagnetic Mn_3 triangles, which all possess appreciable intermolecular interactions, low molecular symmetry, or co-crystallized solvate molecules [15-19]. We observe only subtle differences in the magnetic behavior of $\text{Mn}_3\text{-Cl}$ and $\text{Mn}_3\text{-Br}$; in this letter we treat them as identical.

Magnetic hysteresis measurements were carried out on sub-mm single crystals of $\text{Mn}_3\text{-Cl}$ and $\text{Mn}_3\text{-Br}$, using a high-sensitivity micro-Hall effect magnetometer [24] in the temperature range 0.3-2.6 K. Plots for $\text{Mn}_3\text{-Cl}$ (Fig. 1) of dM/dH vs. the longitudinal field H_L (ie., along the molecular easy axis), at different T, show narrow peaks corresponding to the $k = 0, 1, 2$ and 3 QTM resonances at almost regular field intervals ($\Delta H \sim 0.85$ T). Resonance $k = 1$ (0.85 T) is invisible at low T; it appears only upon application of a transverse field (see Fig. 2), or above 1.5 K, when it appears suddenly at a lower field value (0.80 T). To our knowledge, this is the first time a QTM resonance within a series of resonances is found to be absent [21], while lower and higher resonances are observed. As we show below, this constitutes definite evidence of spin selection rules for QTM.

The observed shift of all resonances to lower fields with increasing T indicates a transition from pure tunneling from the lowest spin level, to thermally activated tunneling between excited states [5]. That excited state resonances appear at lower field values indicates a 4th-order uniaxial anisotropy term in the Mn_3 Hamiltonian (i.e. $B_4^0\hat{O}_4^0$), coming from a relatively weak exchange J between manganese ions (comparable to the single-ion ZFS interaction); the Hamiltonian is then [25]:

$$H = \sum_i (\vec{s}_i \cdot \vec{R}_i^T \cdot \vec{D} \cdot \vec{R}_i \cdot \vec{s}_i - \mu_B \vec{s}_i \cdot \vec{g} \cdot \vec{B}) + \frac{1}{2} \sum_{i,j(i \neq j)} \vec{s}_i \cdot \vec{J} \cdot \vec{s}_j . \quad (1)$$

Here the first term represents the local magnetic anisotropy of the i -th ion, \vec{D} being the ZFS (diagonal) tensor given by $D_{xx} = e$, $D_{yy} = -e$ and $D_{zz} = -d$, with d and e the uniaxial and second order transverse anisotropy parameters, respectively. \vec{R}_i is the Euler matrix specifying the anisotropy axes of the three Mn ions in the molecule, defined by Euler rotation angles α_i , β_i and γ_i . The 2nd term is the Zeeman coupling to the applied field, and the last term is the exchange interaction. The positions of the QTM resonances in both the quantum and thermally activated regimes (Figs. 1-3) can be accurately parametrised by assuming $s_i = 2$, $d = 4.2$ K, $e \sim 0.9$ K, isotropic $g = 2$ and $J = -4.88$ K. The single-ion second order anisotropy (e) is needed to explain the observed QTM rates. Similar d and e values have been reported for Mn^{III} ions elsewhere (eg. Ref. [26]). We also rotated the anisotropy axes for the three Mn^{III} ions such that $\alpha_i = 8.5^\circ$ (with $\gamma_i = 0$), and $\beta_1 = 0$, $\beta_2 = 120^\circ$ and $\beta_3 = 240^\circ$, in order to account for the local tilts of the Jahn-Teller axes and to preserve the C_3 rotation symmetry [13,14].

From the magnetization curve we extract the changes in M at the resonances, to get a rough estimate of the tunnel splittings at each resonance (Fig. 2). At resonance $k = 1$, the splitting ($\Delta_{-6,+5} \sim 1 \times 10^{-6}$ K) is substantially smaller than at resonances $k = 0$ ($\Delta_{-6,+6} \sim 7 \times 10^{-6}$ K), $k = 2$ ($\Delta_{-6,+4} \sim 1 \times 10^{-5}$ K) and $k = 3$ ($\Delta_{-6,+3} > 1 \times 10^{-5}$ K) [27]. We can observe the $k = 1$ resonance by decreasing the field sweep rate (not shown) or by applying a transverse field. The insets to Fig. 2 show the growth of the $k = 1$ peak (lower-right) and the calculated QTM probability [28] at resonances $k = 1$ and $k = 2$ (upper-left) as a function of the transverse field magnitude. The curvature of the probability at $k = 1$ near $H = 0$ indicates saturation, caused by intermolecular dipolar interactions, whose magnitude (~ 250 G) can be estimated from the peak width.

In zero transverse field, the C_3 symmetry of the Mn_3 complexes only allows tunneling between states with $|\Delta m_S| = 3n$. The only resonances observable below the crossover temperature to the pure QTM regime should then be $k = 0$ (tunneling from $m_S = -6$ to $m_S = +6$, $\Delta m_S = 12$) and $k = 3$ (tunneling from $m_S = -6$ to $m_S = +3$, $\Delta m_S = 9$). Exact diagonalization of the Hamiltonian in Eqn. (1) (see Fig. 3) shows that the lowest levels involving the $k = 1$ and $k = 2$ resonances cross exactly, ie., tunneling is forbidden (red circles in Fig. 3), because the spin selection rules are not satisfied (thus, eg., $\Delta m_S = 11$ for ground state QTM at $k = 1$ and $\Delta m_S = 10$ and 8 for the ground and first excited states at $k = 2$). This explains why resonance $k = 1$ only becomes visible at high temperatures in Fig. 1, since an excited state needs to be populated for QTM to take place (eg., the transition from $m_S = -5$ to $m_S = +4$, where $\Delta m_S = 9$). Consequently, the temperature dependence of resonance $k = 1$ constitutes firm evidence for the spin selection rules imposed on QTM in a SMM.

In a finite transverse field, H_T , the symmetry considerations are more subtle. One might also expect resonance $k = 2$ to be absent at low T for small H_T . However this is not the case (see Fig. 3). This can be understood in terms of the tilting of the Jahn-Teller axes of the manganese ions within the molecule, as we see if we now exactly diagonalize the Hamiltonian in Eqn. (1) using the parameters given above [29] for two different cases: a) With the Jahn-Teller axes aligned along the z -axis, i.e. $\alpha = 0$ (thin lines in Fig. 4); and, b) with each Jahn-Teller axes tilted away from the crystallographic z -axis (molecular easy-axis), with the Euler angle $\alpha = 8.5^\circ$ determined from X-ray crystallography data [13,14] (see thick lines and sketch in Fig. 4). In both cases, the tunnel splittings at resonances $k = 1$ and $k = 2$ vanish when $H_T = 0$ (ie., $\Delta_{k=1} = \Delta_{k=2} = 0$) [30]. If the Jahn-Teller axes are

not tilted, large transverse fields ($H_T > 0.2$ T) are required to bring the tunnel splittings up to the experimental magnitudes. However, tilting the Jahn-Teller axes by 8.5° radically alters the transverse field behavior of the ground-state splittings. The finite field splitting of the $k = 0$ and $k = 3$ resonances allowed by symmetry when $H_T = 0$ [30], is mainly generated by the molecular anisotropy, and thus shows weak variation for moderate H_T values. However for the “forbidden” $k = 1$ and $k = 2$ resonances, the transverse field is the only source of level mixing, and this mixing is strongly amplified by the Jahn-Teller tilts. This effect is particularly significant for resonance $k = 2$ (observed at the lowest T), for which a splitting $\sim 10^{-5}$ K is achieved for $H_T < 250$ G, while the ground-state splitting at resonance $k = 1$ is ~ 100 times smaller for the same range of transverse field values. As shown above, intermolecular dipolar interactions can easily provide fields ~ 250 G strong enough to induce a tunnel splitting in the $k = 2$ resonance of the observed value. Meanwhile, their effect on the $k = 1$ resonance is nearly two orders of magnitude weaker, thereby explaining the absence of this QTM step in our studies of carefully aligned crystals (see Fig. 2).

The present results demonstrate the remarkable influence of the molecular symmetry on the magnetic relaxation of molecular nanomagnets, and provide the first clear demonstration of spin selection rules on the QTM for a SMM. The observed behavior must be attributed to the extremely high crystalline quality of these complexes, enabling results that were previously impossible. Of special significance is the remarkable finding that a rotation of the ZFS tensors of the individual ions (in a manner consistent with the crystallographic symmetry) has a profound effect on the transverse field behavior of the tunnel splitting in resonances forbidden by the molecular symmetry.

A small Jahn-Teller axis tilt (8.5°) increases the tunnel splitting value for the $k = 2$ resonance up to an observable level for transverse field magnitudes commonly provided by intermolecular dipolar interactions. The Jahn-Teller axes of individual ions are almost never parallel to each other in *real* structures and thus, according to our results, this combined with dipolar fields and/or disorder is likely the reason for the apparent absence of spin selection rules in previous studies of QTM in SMMs.

ACKNOWLEDGEMENTS:

We gratefully acknowledge fruitful discussions with Eduardo Mucciolo. This work has been supported by the US National Science Foundation (DMR0737802, DMR0747587, DMR0506946, DMR0804408, DMR0239481 and CHE0714488), and by NSERC, PITP, and CIFAR in Canada.

REFERENCES:

1. J.R. Friedman, M.P. Sarachik, J. Tejada, and R. Ziolo, *Phys. Rev. Lett.* **76**, 3830 (1996).
2. L. Thomas, F. Lioni, R. Ballou, D. Gatteschi, R. Sessoli and B. Barbara, *Nature* **383**, 145 (1996).
3. M. Leuenberger, and D. Loss, *Nature* **410**, 789 (2001).
4. D. Gatteschi, R. Sessoli and J. Villain, *Molecular Nanomagnets* (Oxford University Press, New York, 2006)
5. L. Bokacheva, A. D. Kent and M. A. Walters, *Phys. Rev. Lett.* **85**, 4803-4806 (2000).
6. S. Hill, R. S. Edwards, N. Aliaga-Alcade and G. Christou, *Science* **302**, 1015-1018 (2003).
7. W. Wernsdorfer and R. Sessoli, *Science* **284**, 133-135 (1999).
8. A. Cornia, R. Sessoli, L. Sorace, D. Gatteschi, A. L. Barra and C. Daignebonne, *Phys. Rev. Lett.* **89**, 257201 (2002).
9. S. Takahashi, R. S. Edwards, J. M. North, S. Hill and N. S. Dalal, *Phys. Rev. B* **70**, 094429 (2004).
10. E. del Barco *et al.*, *J. Low. Temp. Phys.* **140**, 119-174 (2005).
11. N. V. Prokof 'ev and P. C. E. Stamp, *Rep. Prog. Phys.* **63**, 669-726 (2000).
12. A. Chiolero and D. Loss, *Phys. Rev.* **B56**, 738 (1997).
13. P. L. Feng *et al.*, *Inorg. Chem.* **47**, 8610-8612 (2008).
14. P. L. Feng *et al.*, *Inorg. Chem.* **48**, 3480-3492 (2009).
15. R. Inglis *et al.*, *Chem. Eur. J.* **14**, 9117-9121 (2008).
16. R. Inglis *et al.*, *Chem. Commun.* 5924-5926 (2008).

17. S. G. Sreerama and S. Pal, *Inorg. Chem.* **41**, 4843 (2002).
18. C-I. Yang, W. Wernsdorfer, K-H. Cheng, M. Nakano, G-H. Lee and H-L. Tsai, *Inorg. Chem.* **47**, 10184 (2008).
19. T. C. Stamatatos *et al.*, *J. Am. Chem. Soc.* **129**, 9484 (2007).
20. K. M. Mertes *et al.*, *Phys. Rev. Lett.* **87**, 227205 (2001).
21. In previous investigations of spin selection rules in SMMs [7,20] all QTM resonances were visible: indeed, resonances forbidden by symmetry were comparable in magnitude to the allowed ones. Evidence was extracted mainly from subtle changes in magnitude between them [20], or from their distinct behavior upon application of a transverse magnetic field [7].
22. M. Schechter and P. C. E. Stamp, *Phys. Rev. Lett.* **95**, 267208 (2005).
23. J. Lawrence, E.-C. Yang, R. Edwards, M. M. Olmstead, C. Ramsey, N. S. Dalal, P. K. Gantzel, S. Hill, D. N. Hendrickson, *Inorg. Chem.* **47**, 1965-1974 (2008).
24. A. D. Kent *et al.* *J. Appl. Phys.* **76**, 6656 (1994).
25. Wilson, J. Lawrence, E-C. Yang, M. Nakano, D. N. Hendrickson and S. Hill, *Phys. Rev. B* **74**, 140403(R) (2006).
26. Mantel *et al.*, *J. Am. Chem. Soc.* **125**, 12337-12344 (2003).
27. Tunneling splittings are estimates using the Landau-Zener formalism, and should be considered as lower limits for the low field sweep rates used in the experiment, for which reshuffling of dipolar fields during relaxation can have a significant effect.
28. To study the transverse field dependence of the QTM probability at resonance $k = 1$, the transverse field was applied after sweeping through resonance $k = 0$ in the absence of a transverse field, in order to initialize all measurements from the same magnetic

configuration. Thermal avalanches (extremely frequent in this sample) restricted to a few points our results for resonance $k = 2$, which were obtained by sweeping the magnetic field at different angles with respect to the easy anisotropy axis of the molecules.

29. The observations in Fig. 4 are insensitive to the orientation of the transverse field within the hard anisotropy (x - y) plane over the range of parameter space explored here. This agrees with the absence of any modulation in both the dM/dH peak magnitudes and EPR absorption peak positions (to within the resolution of the techniques).
30. The tunnel splitting of resonance $k = 3$ also vanishes at zero transverse field when the JT axes of the Mn^{III} ions are parallel to z (thin blue line in Fig. 4). The 120° rotations of the single-ion hard/medium axes then generate a molecular 6th-order transverse interaction (i.e. $S_+^6 + S_-^6$), restricting QTM to resonances with $|\Delta m_S| = 6n$. It is the tilt, α , of the Jahn-Teller axes away from the z -axis that imposes the C_3 rotational symmetry of the molecule, lowering the order of the transverse interaction (i.e. $[S_z, (S_+^3 + S_-^3)]$), and allowing QTM resonances with $|\Delta m_S| = 3n$ (thick blue line in Fig. 4).

FIGURES:

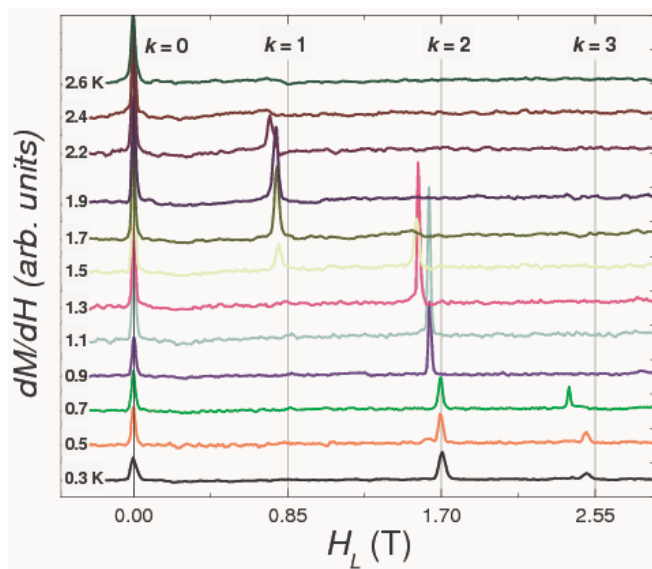


FIG. 1: (Color online) Field derivative of the magnetization curves obtained for a Mn₃-Cl single crystal at different temperatures, with the field swept at 1 T/min along the easy axes of the molecules.

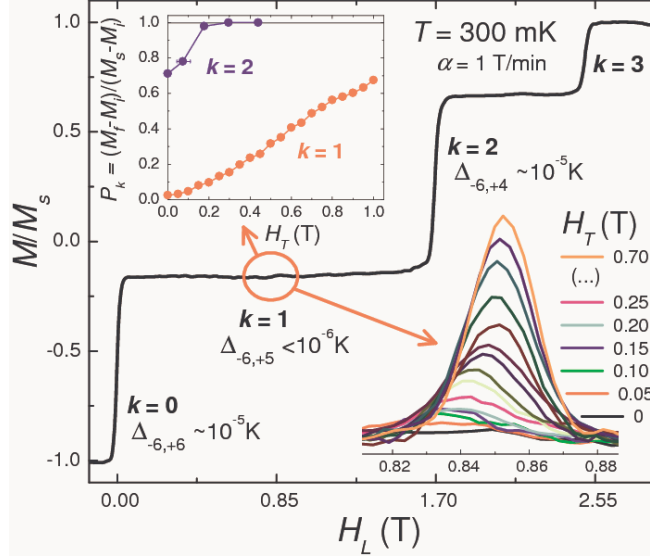


FIG. 2: (Color online) Magnetization versus longitudinal magnetic field recorded at 0.3 K in a $\text{Mn}_3\text{-Cl}$ single crystal. The indicated tunnel splitting values are order of magnitude estimates from the change of magnetization at each resonance [27]. The insets show the increase of the QTM probability at resonances $k = 1$ and 2 (upper-left) and the dM/dH peak at resonance $k = 1$ (lower-right) upon application of a transverse magnetic field.

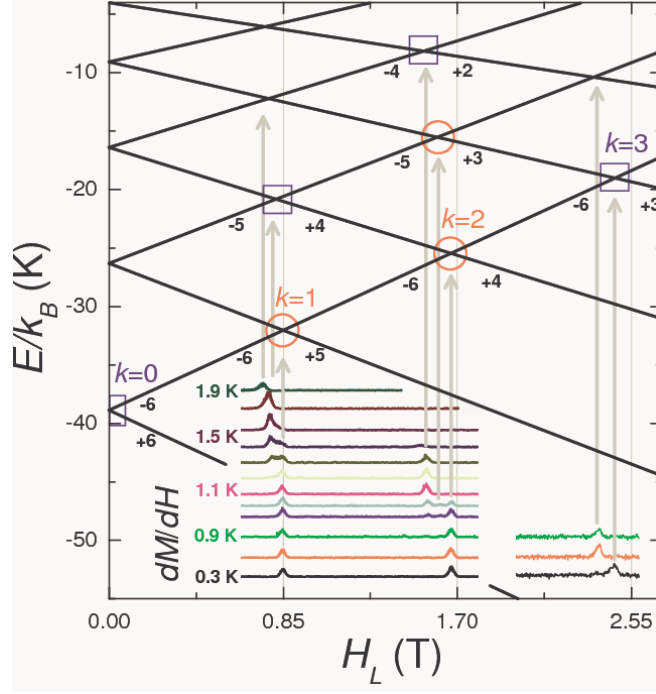


FIG. 3: (Color online) Energies of the Mn_3 m_S levels as a function of the longitudinal magnetic field. Symbols highlight level crossings between different spin states, indicating the degeneracies (red circles) and avoided crossings (blue squares) expected for the C_3 symmetry of the structures. Inset: field derivatives of the magnetization curves (dM/dH_L) measured for a Mn_3 -Br single crystal at different temperatures. Low field sweep rates, 0.05 T/min (data below 1.7 T) and 0.2 T/min (data above 1.7 T), were used to clearly observe and follow the evolution of resonance $k = 1$, which is absent for high sweep rates.

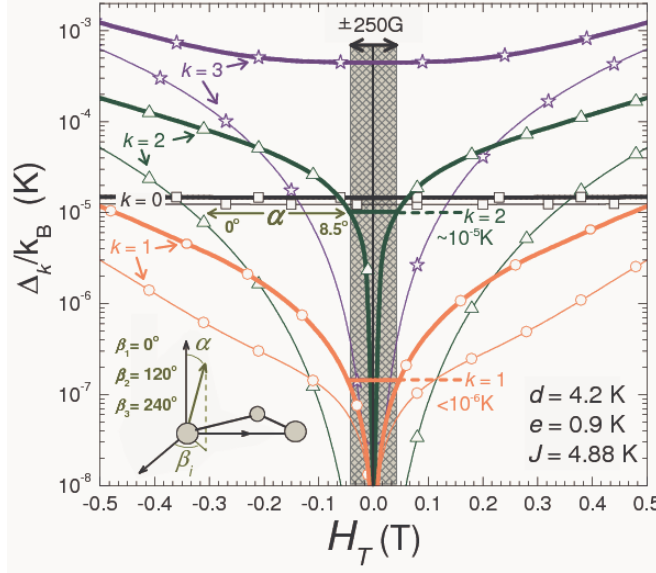


FIG. 4: (Color on-line) Ground state tunnel splittings associated with resonances $k = 0$ (black squares), $k = 1$ (red circles), $k = 2$ (green triangles) and $k = 3$ (blue stars) as a function of the transverse field, H_T , with the Jahn-Teller axes aligned along the z -axis (thin lines) and tilted $\alpha = 8.5^\circ$ away from the z -axis (thick lines). A few symbols per curve have been added to help in their identification. The grey shaded region in the vicinity of zero transverse field represents the strength of the dipolar magnetic field (~ 250 G) felt by the Mn_3 molecules within the single crystal. The horizontal lines within the grey region indicate the order of magnitude of the splitting values attained at resonances $k = 1$ and $k = 2$ for a transverse field of 250 G.